Biochemical Engineering Journal 90 (2014) 214–223

Contents lists available at ScienceDirect

Biochemical Engineering Journal

journal homepage: www.elsevier.com/locate/bej

Regular Article

Modeling of the influence of light quality on the growth of microalgae in a laboratory scale photo-bio-reactor irradiated by arrangements of blue and red LEDs

Ignacio Niizawa [a,b], Josué Miguel Heinrich [a,b], Horacio Antonio Irazoqui [a,b,*]

[a] Group of Innovation on Bio-processes Engineering, Institute for the Technological Development of the Chemical Industry (INTEC), National Council of Scientific and Technological Research (CONICET) and University of Litoral (UNL), Santa Fe, Argentina
[b] Group of Innovation on Bio-processes Engineering, Department of Biochemistry and Biological Sciences (FBCB), University of Litoral (UNL), Santa Fe, Argentina

ARTICLE INFO

Article history:
Received 17 December 2013
Received in revised form 30 April 2014
Accepted 4 May 2014
Available online 15 May 2014

Keywords:
Microalgae
Modeling
Bioreactors
Light Emitting Diode
Monte Carlo
Scale Up

ABSTRACT

Knowing the distribution of the density of radiant energy within a photo-bio-reactor and its impact on the growth of microalgae through the local rate of absorption of radiant energy is essential for the analysis, modeling and design of photo-bio-reactors. In this work we develop a physical model and a computer simulation algorithm, in order to accurately predict the rate of absorption of photons in microalgal cultures at each point of a reactor irradiated with a light source made of different arrangements of LEDs emitting in blue and red spectral regions. Results showed that the average absorption rates in the culture irradiated with blue LEDs were higher than that irradiated with red LEDs. However, the radiation emitted by red LEDs rendered greater energy efficiency for biomass production compared to that emitted by blue LEDs. The development of a computational model based on a Monte Carlo method allowed the determination of the local volumetric rate of photon absorption at each point inside the PBR at different culture times. The information obtained with this tool allowed a detailed assessment of the effect of different radiation conditions on growth of microalgae, regardless of the PBR and the light source used.

1. Introduction

Research on microalgae has grown significantly over the past few decades, due to their multiple uses and applications [1]. Microalgae are photosynthetic microorganisms, which in addition to their need of light, have simple nutritional requirements (CO_2, N, P, K and other micronutrients such as Fe, Mo, etc.). Microalgae can produce large amounts of metabolites in relatively short periods of time [2]. In their cellular structure, they have a large amount of metabolites that have attracted the attention of numerous companies and research groups. Among the metabolites of interest and the different uses of microalgae, we can mention the production of lipids for biofuels of the second generation (biodiesel) [3]; extraction of carotene and other pigments to be used in the pharmaceutical and food industry [4–6], biomass of microalgae as food [7,8] (both for humans as for animals), remediation of gaseous effluents (sequestering of CO_2 emitted by factories or thermal power plants) and of liquid effluents [9], bio-hydrogen production [10], metabolites of microalgae would be feasible for use in therapies against certain diseases [11]; etc.

While the cultivation of microalgae requires simple nutrients (basically they need aqueous solutions of salts, in addition to light), different growing conditions determine different rates of growth, as well as different cell compositions. For example, the use of culture media with different concentrations and sources of nitrogen lead to changes in both the concentration and the profiles of lipids [12]; changes in temperature can affect the rate of growth and the protein content, as well as that of other metabolites [13]; changes in light intensities and the light/dark cycles, have a great influence upon the growth outcomes [14,15]; etc.

Design and construction of a photo-bio-reactor (PBR) for production purposes is a key step in studying growth of microalgae at minor scales (i.e. at bench or laboratory scale and at pilot plant scale). The scaling of a PBR must take into account the influence of the main factors affecting the growth of the microorganism and

* Corresponding author at: Group of Innovation on Bio-processes Engineering, Institute for the Technological Development of the Chemical Industry (INTEC), National Council of Scientific and Technological Research (CONICET) and University of Litoral (UNL), Santa Fe, Argentina. Tel.: +54 342 4575215x172.
E-mail address: hirazo@santafe-conicet.gov.ar (H.A. Irazoqui).

http://dx.doi.org/10.1016/j.bej.2014.05.002
1369-703X/

the final product that is sought. The data collected from the experiments in the laboratory and in the pilot plant must be analyzed and used to ensure proper scaling-up of the reactor.

When an intrinsic model of the rate of growth of microalgae is proposed and then verified in an experimental PBR, it is important to take the light into account as a key aspect, since this is the most important factor affecting the photosynthesis carried out by algae. In general the rate of growth of cultures is limited by the availability of light due to absorption by the culture and dispersion of light by suspended algae. Therefore, knowledge of the distribution of the density of radiant energy within the PBR and its impact on the growth of microalgae through the local rate of absorption of radiant energy is essential for the analysis, modeling and design of a PBR [16].

Light-emitting diodes (LEDs) can be used as artificial light sources in laboratory scale PBRs [17–19]. They have many advantages over other sources of light such as incandescent lamps and fluorescent tubes. These advantages include their small size; their ability to emit in a narrow range of wavelengths; low dissipation of energy as heat; the possibility to adjust the intensity and the wavelength of the emitted light; as well as high efficiency of photoelectric conversion and longer average lifespan [20]. The ability to emit radiation of specific wavelengths make LEDs an ideal tool for carrying out studies on the influence of light quality on microalgae cultures.

The aim of this work is the development of a physical model and a computer simulation algorithm, in order to accurately predict the rate of absorption of photons at each point of a PBR irradiated with light sources made of different arrangements of LEDs emitting in different spectral regions. This configuration allows modification of the emission spectrum by changing the fraction of LEDs that emit at different wavelengths. To validate the simulation programs developed, the predicted values were compared to experimental data. Validated programs are a useful tool for the design and optimization of PBR's, and for studying the influence of light availability and spectral quality on the growth of algae.

2. Materials and methods

2.1. Strain and culture maintenance

The freshwater species *Scenedesmus quadricauda* 276/21 (obtained from CCAP) was grown in 250 ml of BBM culture media [21], frequently used for the cultivation of freshwater microalgae, in 500 ml Erlenmeyer flasks. The cultures were irradiated with fluorescent lamps two weeks prior to use in the PBR experiments.

2.2. Microalgal cultures

A cylindrical PBR of 2 L maximum capacity and 137 cm of diameter was made from borosilicate glass. An air diffuser, consisting of a circular slab made of sintered glass was placed at the center on the PBR's bottom. The bubbles from the diffuser served to mix and aerate the algal suspension. The gas flow is controlled in order to ensure enough gas–liquid transfer area per unit volume as needed to supply the medium with CO_2, to remove the O_2 produced by oxygenic photosynthesis and to ensure the correct agitation of the medium. The temperature was controlled in the range between 25 and 28 °C using a thermostatic bath.

Scenedesmus quadricauda was cultured under different lighting conditions by arranging the LEDs in two different ways in order to assess the effect of the radiation source configuration on the microalgal growth. In the first case, two strips of 24 blue LEDs formed circles around the external wall of the PBR. In the second case, three circles of 24 red LEDs each were fastened to the external wall of the PBR as above. These arrangements are sketched in Fig. 1. Each culture was irradiated with approximately the same number of photons per unit time (Table 1), in order to compare the effects of light quality. The number of photons emitted by the LED arrays was selected so that cultures receive low light intensities.

In both cases 50 ml samples were taken daily during the time of cultivation. Simultaneously, the culture was replenished with the same volume of fresh medium.

Three different cultures were performed independently for each lighting condition (supplementary material section). All three cultures yielded similar results in terms of the concentration of biomass and chlorophyll content.

2.3. Biomass analysis

The algal biomass concentration was followed during growth by measuring the optical density of aliquots of the culture at the 540 nm wavelength (OD_{540}) [22] in a UV–Visible Cary 100 spectrophotometer. At 540 nm there is some absorption of photons by the microalgal suspensions (Fig. 6), however this spectral region is far from the maximum absorption of chlorophylls (about 470 and 680 nm), which makes the measurement less sensitive to possible changes in the chlorophyll content.

The amount of total suspended solids (TSS) [23] was determined for suspensions of different algal concentrations, and the results were correlated linearly with the corresponding values of OD_{540}.

2.4. Chlorophyll analysis

The concentrations of chlorophylls a and b, were determined using the photo-colorimetric technique proposed by Ritchie [24], using 100% ethanol for extraction. The chlorophylls concentrations were correlated with optical densities as follows:

$$\text{Chlorophyll a}\,(\text{mg/L}) = (-5.2007\,OD_{649\,nm} + 13.5275\,OD_{665\,nm})/\text{optical path} \quad (1)$$

$$\text{Chlorophyll b}\,(\text{mg/L}) = (22.4327\;OD_{649\,nm} - 7.0741\,OD_{665\,nm})/\text{optical path} \quad (2)$$

3. Physical and mathematical modeling of the radiant field in the algal suspension

In this study, a stochastic algorithm based on the Monte Carlo method is devised for the simulation of the radiation field in algal suspensions and to predict the local spectral rate of absorption of photons. The algal suspension is modeled as a continuum, where the particles have lost their identity, and have been replaced either by centers of absorption or scattering, randomly distributed throughout the suspension.

Table 1
Type of LEDs, the number of units in each array with the corresponding total rate of emission of photons and the total photon flux density on the external wall of the PBR.

Culture	Number and type of LEDs	Total rate of emission of photons (μmol photons day^{-1})	Total photon flux density (μmol photons m^{-2} sec^{-1})
1	48 blue LEDs	2.126×10^5	38.17
2	72 red LEDs	1.867×10^5	33.52

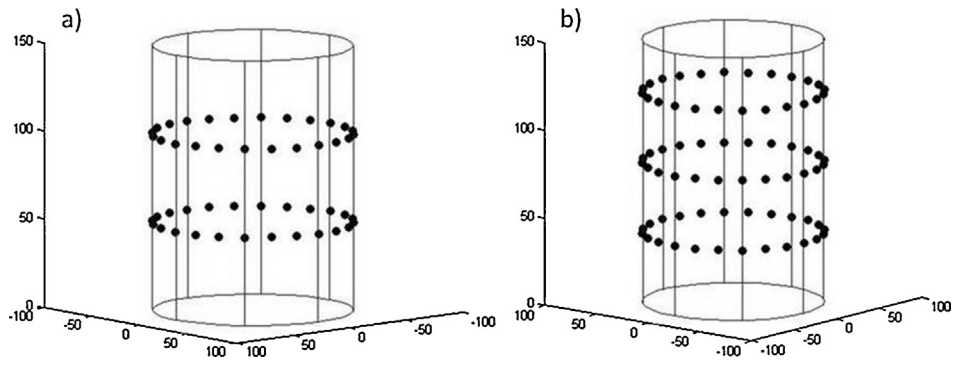

Fig. 1. Photo-bio-reactors with different LED arrangements: (a) culture 1 irradiated with 48 blue LEDs; (b) culture 2 irradiated with 72 red LEDs.

The spectral density of photons which move in a direction $\underline{\hat{\Omega}}$ through every position $\underline{r}$ within the PBR, $n_\lambda(\underline{r}, \underline{\hat{\Omega}}, t)$, is the basic property to be used for the Monte Carlo simulation of the radiant field in a PBR. In this regard, it plays a role equivalent to that of the intensity of the energy beam of wavelength λ, which is propagating in the direction $\underline{\hat{\Omega}}$ through the position $\underline{r}$ ($L_\lambda(\underline{r}, \underline{\hat{\Omega}}, t)$), and these properties are related to one another as follows

$$L_\lambda(\underline{r}, \underline{\hat{\Omega}}, t) = \frac{hc^2}{\lambda} n_\lambda(\underline{r}, \underline{\hat{\Omega}}, t) \tag{3}$$

The unit vector $\underline{\hat{\Omega}}(\theta, \varphi)$ is the direction of motion of a photon, defined by the polar angle θ and the azimuthal angle φ:

$$\underline{\hat{\Omega}}(\theta, \phi) = (1 - \cos^2\,\theta)^{1/2}(\sin\,\phi\underline{\hat{e}}_1 + \cos\,\phi\underline{\hat{e}}_2) + \cos\,\theta\underline{\hat{e}}_3 \tag{4}$$

The spectral density of photons which pass through each position $\underline{r}$, irrespective of the direction of their motion $\underline{\hat{\Omega}}$, is

$$n_\lambda(\underline{r}, t) = \int_{\hat{\Omega}} d\underline{\hat{\Omega}} n_\lambda(\underline{r}, \underline{\hat{\Omega}}, t) = \int_0^{2\pi} d\phi \int_{-1}^{1} d\mu n_\lambda(\underline{r}, \mu, \phi, t) \tag{5}$$

If $n_\lambda(\underline{r}, t)$ is known, the local volumetric rate of photon absorption can be readily obtained [25]:

$$r_\lambda^{\mathrm{abs}}(\underline{r}, t) = c\ \ \alpha_\lambda(t) n_\lambda(\underline{r}, t) \tag{6}$$

where c is the speed of light and α_λ is the spectral absorption coefficient regressed from experimental data in previous work [26].

Knowing $r_\lambda^{\mathrm{abs}}(\underline{r}, t)$ at every location in the culturing medium is key to our understanding of the relative importance of different factors affecting light absorption by microalgae for a given reactor setup, and to compare the performance of different reactor configurations operating under different conditions, regarding this process.

Under good agitation conditions, the cells go from lighted zones to dark zones (and vice versa) many times before cellular replication occurs; therefore, it is reasonable to assume that the kinetics of cell growth is driven by an average rate of photon absorption.

In order to predict the local rate of absorption of photons at every position in the microalgal suspension, the radiant field model must consider the emission characteristics of the source of light and the optical properties of the microalgal culture.

In this work, the Monte Carlo method was employed to simulate the radiation field in a PBR. A schematic of the method is shown in Fig. 2.

The procedure starts with the simulation of the emission of one photon at a time, from the surface of a LED among those arranged as described in Section 2.2. The emission of light by each LED is superficial and isotropic (i.e., the intensity of light is independent of the direction of emission from any point on the surface of a LED). For Monte Carlo simulation purposes, it was assumed that the total rate of emission of photons from all LEDs of one type is proportional to the rate of emission of photons from a single LED of the same type (see Table 1).

The Monte Carlo simulation of the radiant field starts by assigning a direction to every photon at the moment of its emission by a LED. The photon direction of motion is determined by the unit vector $\underline{\hat{\Omega}}(\theta, \varphi)$, which is a function of the polar angle θ and the azimuthal angle φ as indicated in Eq. (4). In the case of a photon at the time of its emission, $\underline{\hat{e}}_3$ is the unit vector normal to the planar surface of the LED; $\underline{\hat{e}}_1$ and $\underline{\hat{e}}_2$ are unit vectors laying on that surface which are perpendicular to each other; θ ranges in the interval $(0,\pi/2)$, while the values of φ are within the interval $(0,2\pi)$.

The energy emitted per unit area of LED, per unit time, within the elementary solid angle $\mathrm{d}\underline{\hat{\Omega}} = \sin\,\theta\,\mathrm{d}\theta\,\mathrm{d}\varphi$ around the direction $\underline{\hat{\Omega}}(\theta, \phi)$, is

$$\begin{aligned} dq_\lambda &= L_\lambda(\underline{\hat{\Omega}})(\underline{\hat{\Omega}} \cdot \underline{\hat{e}}_3) d\underline{\hat{\Omega}} = L_\lambda(\theta, \varphi) \cos\,\theta \sin\,\theta\, d\theta\, d\varphi \\ &= -L_\lambda(\mu, \varphi)\mu\ \ d\mu\, d\varphi \end{aligned} \tag{7}$$

In Eq. (7), $L_\lambda(\underline{\hat{\Omega}})$ is the spectral intensity of light emitted in the $\underline{\hat{\Omega}}(\theta, \phi)$ direction. The energy emitted per unit area of LED, per unit time, per unit solid angle around the $\underline{\hat{\Omega}}$ direction is:

$$f(\theta, \varphi) = \frac{1}{\kappa}\frac{dq_\lambda}{d\underline{\hat{\Omega}}} = \frac{L_\lambda(\theta, \varphi)\cos\,\theta}{\int_0^{2\pi} d\varphi \int_0^{\pi/2} d\theta \cos\,\theta L_\lambda\left(\theta, \varphi\right)} \tag{8}$$

where $\kappa = \int_0^{2\pi} d\varphi \int_0^{\pi/2} d\theta\, \cos\,\theta L_\lambda\left(\theta, \varphi\right)$, is a normalization constant.

In the case of isotropic emission, the spectral light intensity L_λ is independent of the direction of emission and Eq. (8) can be simplified into the following:

$$\begin{aligned} f\left(\theta, \phi\right) &= \frac{\cos\ \theta}{\int_0^{2\pi} d\phi \int_0^{\pi/2} d\theta\ \cos\,\theta} = \left(\frac{\cos\,\theta}{\int_0^{\pi/2} d\theta\ \cos\,\theta}\right)\left(\frac{1}{\int_0^{2\pi} d\phi}\right) \\ &= g(\theta)h(\phi) \end{aligned} \tag{9}$$

where $g(\theta)$and $h(\varphi)$are mutually independent energy distributions on the polar angle θ and the azimuthal angle φ, respectively:

$$g\left(\theta\right) = \frac{\cos\ \theta}{\int_0^{\pi/2} d\theta \cos\,\theta} = \cos\,\theta; \qquad h(\phi) = \frac{1}{2\pi} \tag{10}$$

From Eq. (10), we can conclude that the isotropic emission model is consistent with the angular distribution pattern provided by the manufacturer [28]. For this model, the cumulative probability $P(\theta)$ that a photon is emitted in a direction with polar angle in the interval$(0,\theta)$, is

$$P\left(\theta\right) = \int_0^{\theta} g\left(\theta'\right) d\theta' = \sin\,\theta; \qquad 0 < \theta < \frac{\pi}{2} \tag{11}$$

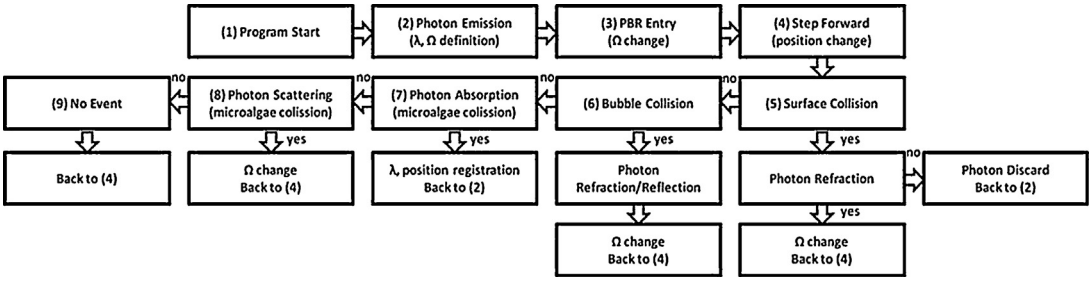

Fig. 2. Computational flowchart including the decision nodes in the stochastic algorithm developed for the Monte Carlo simulation of the radiation field inside the PBR. Details are given in Section 3.

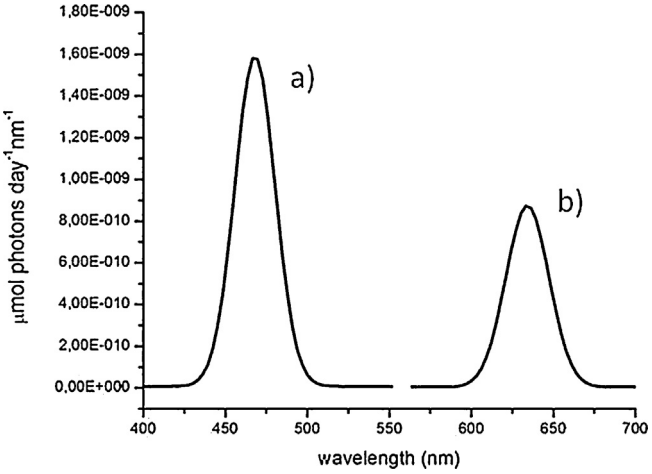

Fig. 3. Emission spectra of N(λ) vs. λ of two types of LEDs: (a) blue (maximum at 470 nm; width at half maximum: 30 nm) and (b) red (maximum at 630 nm; width at half maximum: 31.5 nm).

Similarly, the cumulative probability $P(\varphi)$, that a photon is emitted in a direction with azimuthal angle in the interval (0,φ)is

$$P(\varphi) = \int_0^{\varphi} g(\varphi')d\varphi' = \frac{\varphi}{2\pi}; \qquad 0 < \varphi < 2\pi \tag{12}$$

In the context of the Monte Carlo algorithm, $P(\theta)$ and $P(\varphi)$ are replaced with the random numbers δ_θ and δ_φ in the interval (0,1).

The distribution of the number of photons emitted per unit time as a function of their wavelength is a characteristic of each type of LED. Such spectral distributions corresponding to the blue and red LEDs used in this work, provided by the manufacturer [28] are shown in Fig. 3.

The spectral intensity $L_\lambda(\hat{\Omega})$ of a beam of light emitted by a LED in the direction $\hat{\Omega}$, actually is the distribution with respect to wavelength, of the emitted energy carried by the beam and enclosed by the elementary solid angle $d\hat{\Omega}$ around the $\hat{\Omega}$ direction. Therefore, the product $L_\lambda(\hat{\Omega})d\lambda$ is the fraction of emitted energy in the direction $\hat{\Omega}$ with wavelengths between λ and $\lambda + d\lambda$. In the case of isotropic emission, like ours, the product $L_\lambda d\lambda$ is the fraction of emitted energy in any direction with wavelengths between λ and $\lambda + d\lambda$.

Considering that the energy of a photon of wavelength λ is $h(c/\lambda)$, the relationship between the flux density of energy, dq_λ, emitted around the direction $\hat{\Omega}(\theta, \phi)$ by a LED with an isotropic emission pattern and the corresponding flux density of photons, $d\dot{n}_\lambda$, becomes apparent:

$$d\dot{n}_\lambda = \left(\frac{\lambda}{hc}\right) L_\lambda \cos\ \theta \sin\theta\, d\theta\, d\varphi = -\left(\frac{\lambda}{hc}\right) L_\lambda \mu \quad d\mu\, d\varphi \tag{13}$$

Integration over all directions of emission gives the total flux of emitted photons of wavelength within the elementary interval between λ and $\lambda + d\lambda$:

$$\dot{n}_\lambda = \pi \left(\frac{\lambda}{hc}\right) L_\lambda \tag{14}$$

In Eq. (14), $\dot{n}_\lambda$ and L_λ are the distribution functions with λ of the total flux density of emitted photons and of the isotropic intensity, respectively.

The distribution of the number of photons emitted per unit time, either by a red LED or by a blue one, as a function of λ is $\dot{N}(\lambda) = A_L \dot{n}_\lambda$, where the surface of each LED is A_L. The profiles of $\dot{N}(\lambda)$ vs. λ, for blue and red LEDs provided by the manufacturer [28], are shown in Fig. 4. A wavelength is assigned to every emitted photon according to the spectral emission characteristics of the radiation source. The spectral output of the source of photons can be built on the basis of the emission distribution of each type of LED, together with each particular source design among those already discussed in Section 2.2.

The cumulative probability that a photon is emitted with a wavelength within the interval (0,λ), regardless of its direction of emission, is

$$P(\lambda) = \frac{\int_0^{\lambda} \dot{N}(\lambda')\, d\lambda'}{\int_0^{\infty} \dot{N}(\lambda)\, d\lambda} \tag{15}$$

where $\dot{N}(\lambda)$ is the appropriate distribution function for each type of LED. In the Monte Carlo algorithm, $P(\lambda)$ is replaced with the random number δ_λ in the interval (0,1).

Within a homogeneous culturing medium, the attenuation of the intensity of a beam of light is caused by the absorption of light by pigments of microalgae, and by scattering of the beam into different new directions, when it interacts with the suspended cells (it is considered that the scattering is due only to the microalgal suspension because only water, inorganic ions and small molecules are present in the culture medium). In order to build a stochastic model of the radiant field in homogeneous suspensions of microalgae, it is necessary to assign probabilities to the occurrence of the phenomena of absorption and of dispersion (i.e., of photon scattering). The probabilities $P(A)$ and $P(S)$ of these events were modeled in previous work, and their relationship with the spectral absorption coefficient α_λ, as well as with the scattering coefficient ξ_λ, was established [26] and verified [27]. To tell whether a photon is absorbed or scattered, or if it flies freely for an elementary distance Δs in its current direction of motion through the homogeneous suspension, a random number δ_{motion}, $0 < \delta_{\text{motion}} < 1$, is generated and it is compared with $P(A)$ and $P(S)$. If $0 < \delta_{\text{motion}} < P(A)$, it is assumed that the photon is absorbed; if $P(A) < \delta_{\text{motion}} < P(S)$ it is assumed that the photon is scattered into a new direction, and if $P(A) + P(S) < \delta_{\text{motion}}$ it is assumed that the photon flies the elementary distance Δs uneventfully, as long as this elementary step is entirely within the homogeneous suspension.

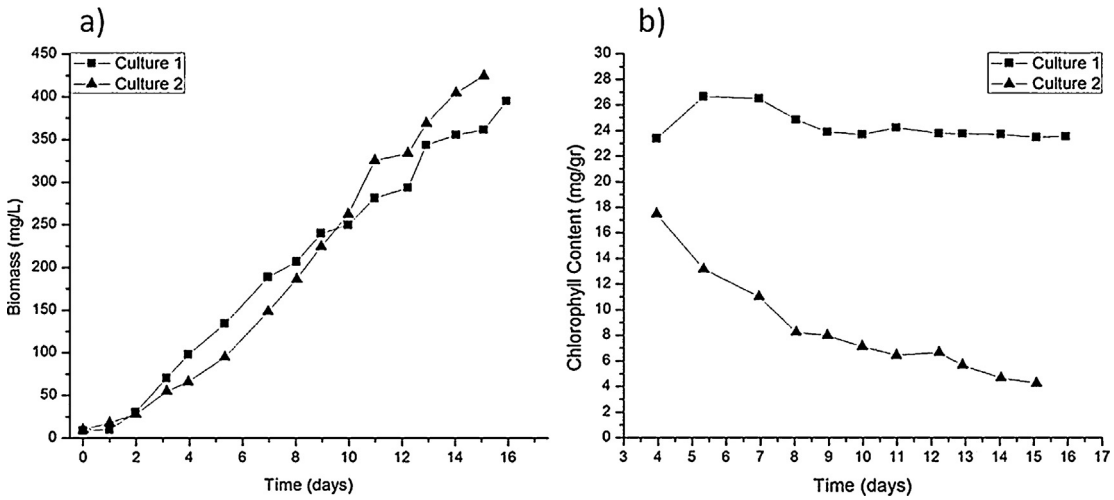

Fig. 4. Cultures of *Scenedesmus quadricauda* in a PBR irradiated with arrays of blue and red LEDs: (a) biomass concentrations vs. time, and (b) the contents of pigments (chlorophylls) per unit dried weight of algae vs. time.

In the case that the photon is scattered by the suspended cells, a transition from its original direction $\hat{\Omega}$ into a new one, $\hat{\Omega}'$, occurs. The probability distribution of this transition, which is conditional in the sense that it is assumed that photon scattering by suspended cells has already happened, is given by the phase function $B(\hat{\Omega}\cdot\hat{\Omega}')$. The phase function is axially symmetric about the original direction of motion $\hat{\Omega}$, depending only on the dot product $\mu=\hat{\Omega}\cdot\hat{\Omega}'$. It satisfies the normalization condition

$$\frac{1}{4\pi}\int_{\hat{\Omega}'} d\hat{\Omega}' B(\hat{\Omega}\cdot\hat{\Omega}') = \left[\frac{1}{2\pi}\int_0^{2\pi} d\varphi\right]\left[\frac{1}{2}\int_{-1}^{1} d\mu B(\mu)\right] = 1 \quad (16)$$

A model of the phase function $B(\hat{\Omega}\cdot\hat{\Omega}')$ was proposed in a previous paper [27]. The cumulative conditional probability that after suffering a scattering event, the photon has a new direction (φ',μ'), with φ' within the interval (0,φ) and μ' within the interval (-1,μ), is

$$P(\varphi,\mu) = P(\varphi)P(\mu) = \left[\frac{\varphi}{2\pi}\right]\left[\frac{1}{2}\int_{-1}^{\mu} d\mu' B(\mu')\right] \quad (17)$$

In the Monte Carlo algorithm, $P(\varphi)$and $P(\mu)$ are replaced with random numbers $\delta\varphi$ and $\delta\mu$ in the interval (0,1), respectively.

An air diffuser, consisting in a circular slab made of sintered glass, was placed at the center of each PBR's bottom. From the gas diffuser, a swarm of bubbles rises through the algal suspension, which serves the purpose of mixing the medium; supplies CO_2 to the culture, and removes the O_2 produced by oxygenic photosynthesis. These bubbles are contained in a region enclosed by an inverted cone, with its apex at the center of the diffuser. It was assumed that bubbles are spherical, with a homogeneous distribution of their radius around the mean value. When a photon, which is being tracked with Monte Carlo stochastic techniques, enters this non-homogeneous region, chances are that it may collide with a bubble. The probability of collision between a photon and a bubble, when the photon moves an elementary distance Δs in any direction through the non-homogeneous medium, is assessed as proposed by Heinrich et al. [25]:

$$P(s) = \left[1-\exp\left(-\frac{\Delta s}{\bar{s}_b}\right)\right] = \left\{1-\exp\left[-\left(\frac{3}{4}\right)\theta_G\frac{\Delta s}{\bar{r}_b}\right]\right\} \quad (18)$$

In Eq. (18), $\bar{s}_b$ is the average of the free flight distances of the photon computed over the ensemble; $\bar{r}_b$ is the mean radius of the bubbles;$\theta_G=(2V_G/V_L+V_G))$ is the gas volume fraction in the zone with bubbles; V_G is the total gas volume resident in the reactor (gas holdup), and (V_L+V_G) is the reactor total volume.

When a photon collides with a bubble, it is either reflected back toward the suspension or it is refracted into the gas phase, thus changing its direction according to Snell's law. In the latter case, the photon will follow a straight trajectory inside the bubble until it hits again the surface of the bubble, this time from the gas side. At this point, it can be reflected back toward the gas phase or transmitted and refracted into the surrounding suspension. A similar situation occurs when a photon hits a wall of the reactor: here again it can be reflected or transmitted through the wall. If the latter of these events happens, the photon exits the medium and is removed from the radiation field, whereas if reflected, it will remain in the field with a new direction according to Fresnel reflection law:

$$\rho_{1,2}(\hat{\Omega},\hat{\Omega}',\hat{n}) = \frac{1}{2}\left[\frac{\eta_1(\hat{n}\cdot\hat{\Omega})-\eta_2(\hat{n}\cdot\hat{\Omega}')}{\eta_1(\hat{n}\cdot\hat{\Omega})+\eta_2(\hat{n}\cdot\hat{\Omega}')}\right]^2 + \frac{1}{2}\left[\frac{\eta_1(\hat{n}\cdot\hat{\Omega}')-\eta_2(\hat{n}\cdot\hat{\Omega})}{\eta_1(\hat{n}\cdot\hat{\Omega}')+\eta_2(\hat{n}\cdot\hat{\Omega})}\right]^2 \quad (19)$$

In Eq. (19), $\rho_{1,2}$ is the reflectivity on the interface between phases 1 and 2; $\hat{\Omega}$ and $\hat{\Omega}'$ are unit vectors in the direction of incidence and of reflection on that interface, respectively; η_1 and η_2 are the indices of refraction of phases 1 and 2; and $\hat{n}$ is the unit normal vector to that interface, pointing toward either of the two phases. To tell whether a photon is reflected or transmitted, a random number δ, $0<\delta_{ref}<1$, is generated and it is compared with $\rho_{1,2}$. If $0<\delta_{ref}<\rho_{1,2}$, it is assumed that the photon is reflected according to Fresnel law; otherwise it is assumed that the photon is transmitted through the boundary and removed from the radiant field.

The effects of the probes and control devices (temperature sensor, sampling port, air diffuser, etc.) on the radiation field have been neglected. Successively, the trajectory of a sufficiently large number of photons is simulated as they travel through each of the reactor sectors, until their eventual end. One by one, photons are emitted from the LEDs in a succession. Although during the execution of the computational algorithm, photons are individually emitted in a succession, together they simulate the radiation field properties inside the reactor at each stage of growth. The radiation field properties adjust themselves without delay to the evolution with time of the microalgae culture through a continuous succession of steady states.

4. Results and discussion

4.1. Microalgal cultures

In Fig. 4, for (a) biomass concentrations vs. time and (b) the contents of pigments (chlorophylls) per unit dried weight of algae vs. time.

Although the growth curves intersect at about the ninth day of cultivation, the biomass concentrations at different times in culture 1 (irradiated with blue LEDs) were similar to those in culture 2 (irradiated with red LEDs) (Fig. 4a). Each culture was irradiated with approximately the same number of photons per unit time (2.126×10^5 and 1.867×10^5 μmol photons day^{-1}, respectively). However, the chlorophylls content per unit biomass was always greater in culture 1 than in culture 2 (Fig. 4b).

Blue and red LEDs used in this work emit photons which are more energetic than the excitation energy of both, photosystem II (P680) and I (P700). Photons in the blue light region may excite the primary absorbing chromophore to its second, short lived singlet state and, among other possibilities, the excitation energy may be re-emitted by fluorescence. After the photons emitted either by blue or red LEDs have been captured, their excess energy can also be dissipated as heat through a stepwise process to reach the first singlet state of the absorbing chromophore.

The return of excited chlorophylls from the first singlet to the ground state may proceed stepwise, by going through many vibrational and rotational energy levels, and eventually dissipate the excitation energy into thermal energy, which is lost to a thermal sink. This returning to the ground state can also occur by sharing excitation energy with a neighboring chromophore molecule. When chromophores are positioned in a specific way due to their binding with supporting proteins and very close to each other, the quantum of energy of an absorbed photon can be transferred from a chromophore in the antenna to a neighboring one via exciton transfer. By this transfer mechanism the excitation energy of captured photons is partly transferred through the antennae to their corresponding reaction centers and also, in this process, is partly degraded to thermal energy [29].

The excitons relayed to the reaction center cause a charge separation. The velocity of the exciton transfer process in the antennae is much faster than that of charge separation in the reaction center. The latter is the rate controlling step of the overall photon absorption and exciton transfer process that ends with the excitation of a pair of closely adjacent chlorophylls-a located at the reaction center (the “special pair”), which finally transfers an electron to a neighboring acceptor [30].

Collectively, excitons function as energy pools in the antennae, which deliver energy to the reaction center of their respective photosystem (i.e., either to P680 or P700) at a low speed compared to that of exciton transfer between neighboring chromophores. The instantaneous amount of energy resident in the antenna complexes depends on the intensity of the incident radiation, and on the mechanism of exciton distribution between the two photosystems [31].

Altogether, with all these processes put into play the energy of the absorbed photons whose wavelengths were from the blue spectral zone up to 680 nm, is transported via exciton transfer to the reaction center of PSII and PSI and optimally distributed between them. These centers require sharply defined excitation energies (corresponding to wavelengths of 680 and 700 nm), and the exciton energy in excess must be degraded as heat, while the excitons with energy below the threshold could be completely converted into thermal energy. From the end of the exciton transfer process, it is not possible to trace back the energy quality of the light that caused it [32]. This could explain why the biomass concentrations at different times in the crop irradiated with blue LEDs (emission maximum at 470 nm) were similar to those of the crop irradiated with red LEDs (emission maximum at 630 nm), when each culture was irradiated with approximately the same number of photons per unit time.

The lower efficiency of blue light for algal biomass production compared to that resulting from of red light (see Fig. 8a and b), could be attributed to the process of light absorption, followed by exciton transfer in the antennae, occurring before the excitation of the reaction centers. In Fig. 8a, the percentage of all photons emitted by the LED arrays, that are absorbed by culture 1 (blue LEDs) and 2 (red LEDs) are reported at different times of growth.

After the eleventh day of the culture, about 80% of the photons emitted by the blue LEDs are absorbed, while in the case of the red LEDs only 20% of the total emitted photons are absorbed. As shown in Fig. 4b the prevalent absorption of blue photons compared to that of red photons, is accompanied by a larger content of chlorophylls in the biomass at all times during the experiment. Because the respective growth curves are quite similar, it can be speculated that those excitons generated from the most energetic photons, have been quenched into thermal energy with preference over those emitted by red LEDs.

4.2. Analysis of the radiant field in the PBR

The local volumetric rate of photon absorption in culture 1 (irradiated with blue LEDs) and in culture 2 (irradiated with red LEDs), $r^{abs}_{PAR}(\underline{r}, t)$, which are the result of summing up all the contributions within the photosynthetically active spectral zone, are shown in Figs. 5 and 6, at different radial positions and at different times, where:

$$r^{abs}_{PAR}(\underline{r}, t) = \int_{400}^{700} r^{abs}_{\lambda}(\underline{r}, t)d\lambda \tag{20}$$

In the culture illuminated by blue LEDs the values of $r^{abs}_{PAR}(\underline{r}, t)$ increase markedly with biomass concentration in the region adjacent to each LED, while they decrease or even remain almost constant in the rest of the reactor (Fig. 5). Furthermore, in the culture illuminated with red LEDs, the values of $r^{abs}_{PAR}(\underline{r}, t)$ increase in the bulk of the reactor as the biomass concentration increases. The reason for this could be that the lower chlorophyll content of the culture illuminated by red LEDs allows the photons to travel greater distances in the suspension before being absorbed (Fig. 6), so that the values of $r^{abs}_{PAR}(\underline{r}, t)$ are more evenly distributed throughout the reactor. At low concentrations of biomass, and therefore at low rates of absorption, photons can travel distances large enough to cause light to be concentrated at the core of the reactor, where $r^{abs}_{PAR}(\underline{r}, t)$ can reach a local maximum, as shown in Fig. 6d.

The absorption coefficient, α_{λ}, of a culture of microalgae determines its ability to capture photons from the radiant field that propagates through it. The coefficient value depends on both the concentration of microalgae in the culture and the chlorophyll content per unit biomass. Therefore, cultures with higher biomass concentration but lower chlorophylls content could show photon absorption rates smaller than those of less concentrated cultures, but with higher chlorophylls content. The developed program allows an accurate simulation of the interaction between the radiation field and the culture of microalgae, expressed as the wavelength dependent, local rate of photon absorption. The simulation program takes into account the quality and the intensity of the radiation emitted by the light source, as well as its configuration.

4.3. Average rate of photon absorption

The number of incident photons per unit of irradiated surface and per unit time (i.e., the photon flux density on that surface),

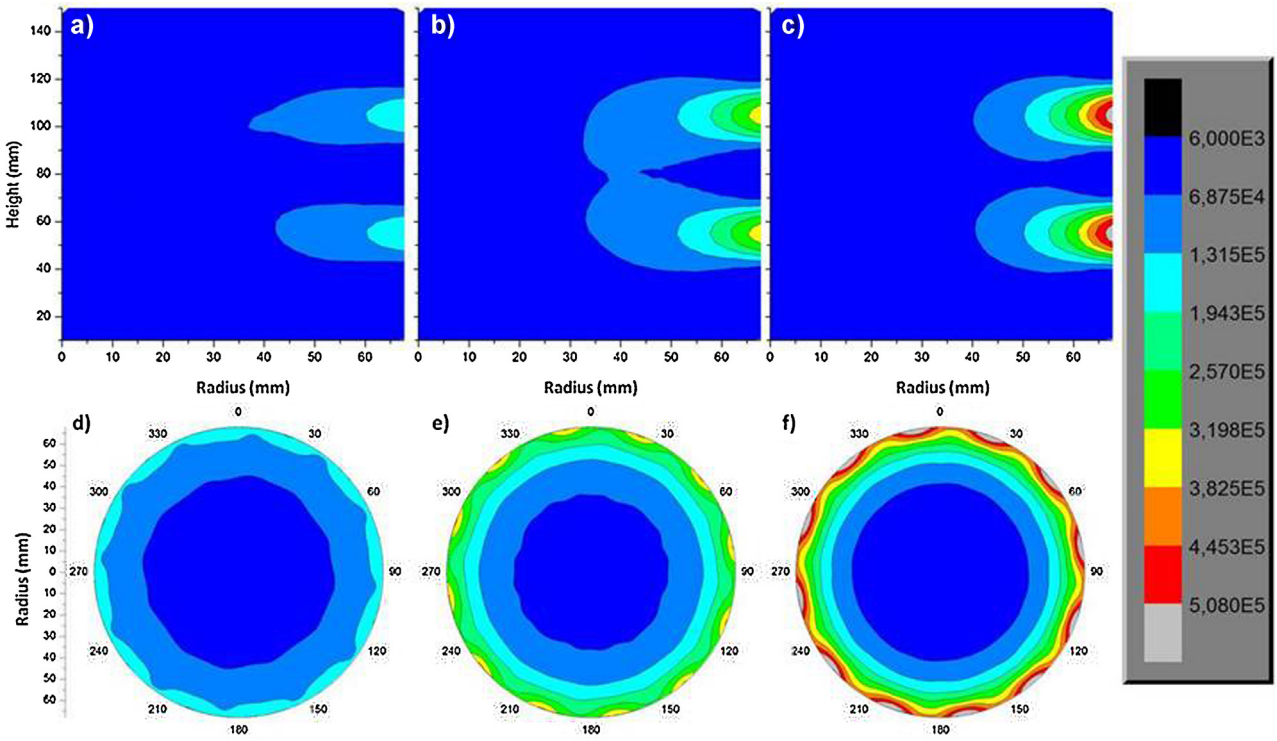

Fig. 5. $r^{abs}_{PAR}(\underline{r}, t)$ profiles depending on the radius and height of the reactor, (a), (b) and (c), and as function of the radius and the height at which the LEDs are located (d, e, f) for the cultivation 1 days 7, (a) and (d); 10, (b) and (e), and 20, (c) and (f). To the right graph shows the values taken according to graph colors expressed in units of μmol of photons * L^{-1} * day^{-1}.

is often used as the basis of comparison in studies regarding the effects of the properties of the radiation field on the growth of microalgae. However, this boundary condition alone cannot uniquely determine the distribution of light in the bulk of a culture of microalgae, nor the local rate of absorption of photons. Due to the inherent non-uniformity of the light distribution in an algal suspension, in most cases it is necessary to know the local rate of absorption of photons of photosynthetically active wavelengths,

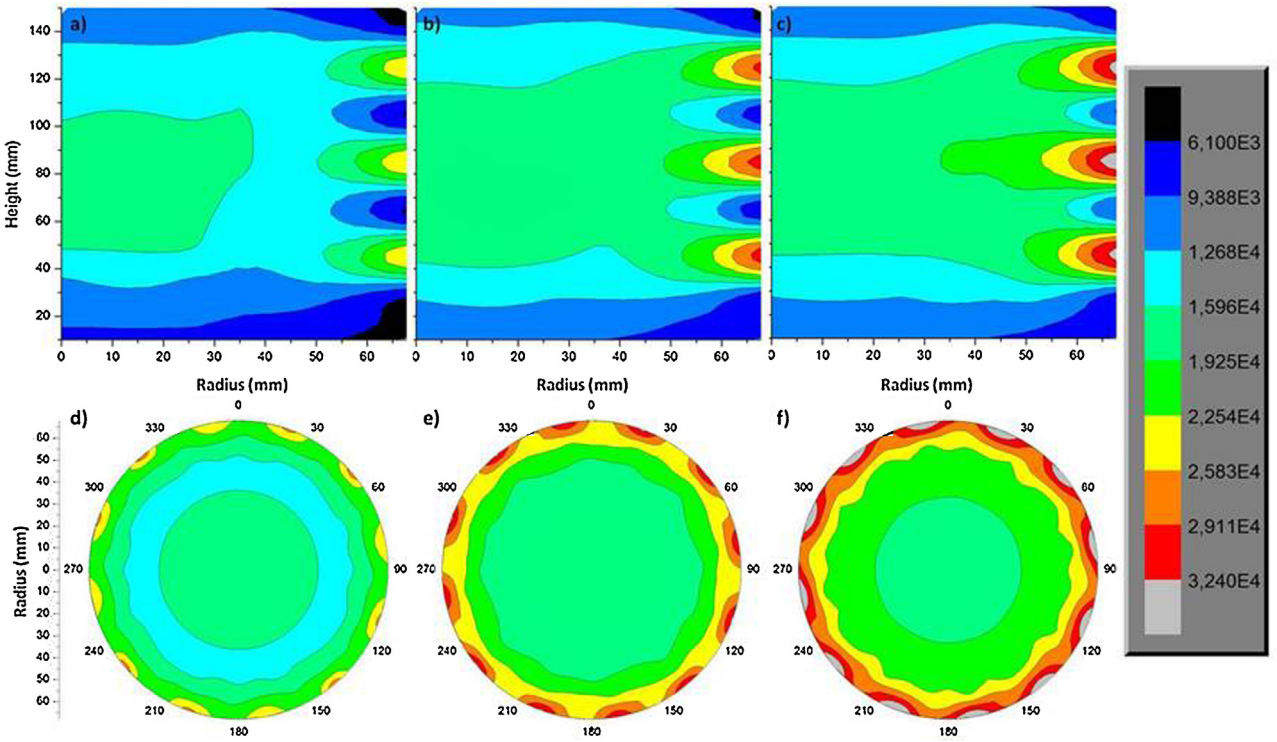

Fig. 6. $r^{abs}_{PAR}(\underline{r}, t)$ profiles depending on the radius and height of the reactor, (a), (b) and (c), and as function of the radius and the height at which the LEDs are located (d, e, f) for the cultivation 2 days 12, (a) and (d); 16, (b) and (e), and 20, (c) and (f). To the right graph shows the values taken according to graph colors expressed in units of μmol of photons * L^{-1} * day^{-1}.

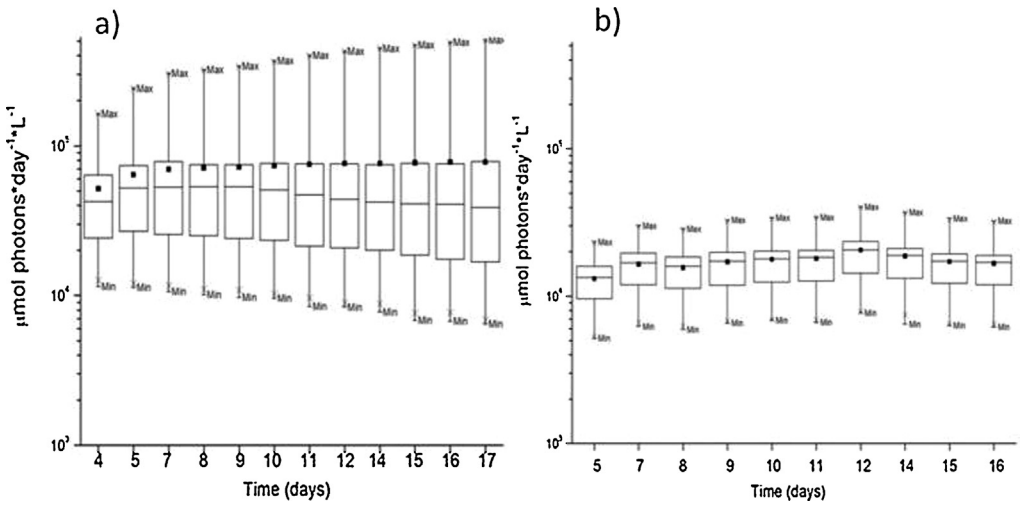

Fig. 7. Box diagrams showing the dispersion of the values of $r^{abs}_{PAR}(\underline{r}, t)$ in the laboratory scale PBR. (a) Culture 1; (b) Culture 2. With ■, the time-dependent average value of $r^{abs}_{PAR}(\underline{r}, t)$ is indicated. The values are expressed on a logarithmic scale of µmole photons day^{-1} L^{-1}.

$r^{abs}_{PAR}(\underline{r}, t)$, as a prerequisite for a systematic comparison of different PBR configurations, and to optimize its operating conditions, as well as to change the scale from the laboratory to a pilot plant or to a production unit. An unfavorable situation could be conceived in which, after a given time of growth, a stratification of the light in the reactor occurs to the extreme that large portions of the suspension no longer receive enough light for active photosynthesis, turning them into dark zones. Under these conditions the reactor operates as if reactors of different sizes coexist, each corresponding to one of the different wavelengths of the light making up the radiation field.

For the simulation of the local rate of photon absorption, the volume of the laboratory scale reactor was divided into elementary cells of equal size, and a value of $r^{abs}_{PAR}(\underline{r}, t)$ predicted by simulation was assigned to each of these elementary volumes. The box diagrams of Fig. 7, show the dispersion of the values of $r^{abs}_{PAR}(\underline{r}, t)$ in the volume of the laboratory scale reactor, as a function of the time of growth.

According to the box diagrams of Fig. 7a, the greater dispersion of the values of $r^{abs}_{PAR}(\underline{r}, t)$ about the average is found in culture 1 (blue LEDs). In this case the high $r^{abs}_{PAR}(\underline{r}, t)$ values in the regions adjacent to the LEDs (Fig. 5) produce higher values $r^{abs}_{PAR}(t)_{average}$, compared to those of culture 2 (red LEDs) (Fig. 7b), while causing greater dispersion of the values of $r^{abs}_{PAR}(\underline{r}, t)$ around those regions because the local rate of photon absorption is much lower in most of the culture volume.

In culture 2, $r^{abs}_{PAR}(t)$ values are more evenly distributed throughout the culture due to the low concentrations of chlorophyll per unit biomass, causing both the average of $r^{abs}_{PAR}(t)$ values and their dispersion to be smaller than in culture 1 (Fig. 6).

A wide dispersion of $r^{abs}_{PAR}(t)$ values about the average in a culture, is indicative of a degree of stratification of light in the microalgal suspension.

4.4. The energy efficiency of PBRs

In order to evaluate the photosynthetic efficiency of each type of radiation for the cultivation of microalgae, it is important to consider both the energy emitted and the energy absorbed by microalgae and their subsequent use for growth. For this, the total power emitted by the arrays of LEDs, $E_{emitted\ light}$, is calculated based on the emission profile of each type of LED (Fig. 4),

$$E_{emitted\ light}(J\ day^{-1}) = hc \int_{\lambda} q_{\lambda} \frac{d\lambda}{\lambda} \tag{21}$$

together with the calculation of the energy absorbed, $E_{abs\ light}$, by microalgae based on the local $r^{abs}_{\lambda}(\underline{r}, t)$ values in each culture

$$E_{abs.\ light}(Jday^{-1}) = hc \int_{\underline{r}} \int_{\lambda} r^{abs}_{\lambda}(\underline{r}, t) \frac{d\lambda}{\lambda} d\underline{r} \tag{22}$$

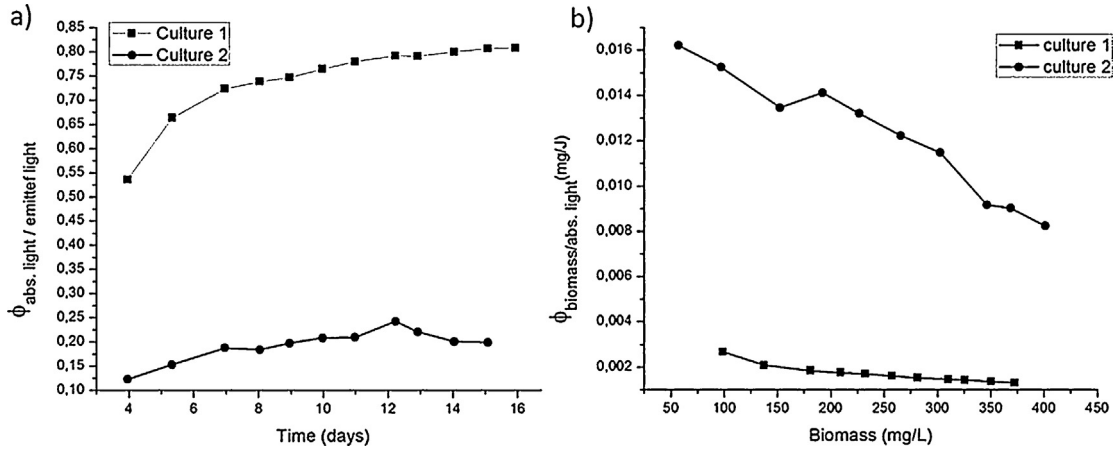

Fig. 8. (a) Fraction of energy absorbed per unit energy emitted by each type of LEDs, (b) efficiency of biomass production per unit of energy absorbed by microalgae.

Then, the absorbed fraction of the total energy emitted by each type of LEDs, $\phi_{(\text{abs. light/emitted light})}$, is assessed (Fig. 8a)

$$\phi_{(\text{abs. light/emitted light})} = \frac{E_{\text{abs. light}}}{E_{\text{emitted light}}},$$

as well as the efficiency of the absorbed light of each quality regarding biomass production, $\phi_{(\text{biomass/abs. light})}$,

$$\phi_{(\text{biomass/abs. light})} = \frac{\Delta M_{\text{biomass}}}{E_{\text{abs. light}}} \quad (23)$$

which is shown in Fig. 8b.

It is noted that the radiation emitted by the red LEDs is more efficient than that of the blue LEDs in both the absorption process and in the production of biomass per unit of energy absorbed over the entire range of biomass concentrations explored.

5. Conclusions

Results showed that the average absorption rates in the culture irradiated with blue LEDs were higher than that irradiated with red LEDs (Fig. 7). However, the dispersion around their respective average values was much higher in the first case, due to the fact that higher concentrations of microalgal chlorophylls (Fig. 4b) cause a larger fraction of photons absorbed in regions adjacent to the LEDs (Fig. 5) giving rise to dark zones at the center of the PBR where low irradiation levels might not be sufficient to maintain algal growth. This wider dispersion of the values of the rate of photon absorption about the average may raise uncertainties about the reliability of conclusions regarding the effectiveness of the interaction between the radiant field and suspended microalgae, when they are only based on data of average absorption rates, $r^{\text{abs}}_{\text{PAR}}(t)_{\text{average}}$.

As show in Fig. 8a smaller number of photons are absorbed in culture 2 because of the lower values of α_λ. However, the radiation emitted by red LEDs rendered greater energy efficiency for biomass production compared to that emitted by blue LEDs (Fig. 8b).

The decrease of chlorophyll content in culture 2 might be due to light quality, but also could be indicative of photo-inhibition [33]. The total photon flux density values in Table 1 are expressed as the total rate of emission of photons by the LEDs over the entire lateral wall of the reactor. Although these values are much lower than those reported for photo-damage [34], the values of the spectral density of photons in comparatively small regions near the LEDs are higher than those reported in Table 1. However, under good agitation conditions, cells switch between zones with different photon densities many times before cellular replication occurs. The residence time of the cells in each of these zones will be proportional to the fraction of the total volume spanned by each zone. Therefore, it is reasonable to assume that the kinetics of cell growth is driven by an average rate of photon absorption and not by a local ones. More research is required to confirm these speculations, but this is beyond the scope of the present work.

Predicting the local rate of photon absorption, $r^{\text{abs}}_{\lambda}(\underline{r}, t)$, requires knowing the spectral coefficient of absorption, α_λ, and the local density of photons, n_λ, at every position in the PBR (Eqs. (5) and (6)). The local density of photons is predicted by means of Monte Carlo simulation using the absorption coefficient, α_λ, and the scattering coefficient, ξ_λ, obtained in a previous paper [26] by regression from experimental data on microalgal cultures.

The methodology used in this paper allows a detailed assessment of the effect of different irradiation conditions and different reactors configurations on microalgal growth.

Acknowledgements

Funds were provided by Universidad Nacional del Litoral, CAI+D Redes No. 9 Reactores y Procesos Biológicos para la Producción de Microorganismos Sustitutos de Agroquímicos y para la Obtención de Materias Primas Alternativas para la Fabricación de Biocombustibles and Consejo Nacional de Investigaciones Científicas y Técnicas de la República Argentina (CONICET) PIP IU Modelado y optimización de foto-bio-reactores destinados al cultivo de microorganismos fototróficos para diferentes aplicaciones biotecnológicas.

Appendix A. Supplementary data

Supplementary material related to this article can be found, in the online version, at http://dx.doi.org/10.1016/j.bej.2014.05.002.

References

[1] T.M. Mata, A.A. Martins, S. Nidia, Caetano, Microalgae for biodiesel production and other applications: a review, Renew. Sust. Energy Rev. 14 (2010) 217–232.
[2] L. Brennan, P. Owende, Biofuels from microalgae: a review of technologies for production, processing, and extractions of biofuels and co-products, Renew. Sust. Energy Rev. 14 (2010) 557–577.
[3] Y. Chisti, Biodiesel from microalgae, Biotechnol. Adv. 25 (2007) 294–306.
[4] J. Fábregas, A. Domínguez, M. Regueiro, A. Maseda, A. Otero, Optimization of culture medium for the continuous cultivation of the microalga *Haematococcus pluvialis*, Appl. Microbiol. Biotechnol. 53 (2000) 530–535.
[5] D.H. Zhang, Y.K. Lee, M.L. Ng, S.M. Phang, Composition and accumulation of secondary carotenoids in *Chlorococcum* sp, J. Appl. Phycol. 9 (1997) 147–155.
[6] B.F. Cordero, I. Obraztsova, I. Couso, R. León, M.A. Vargas, H. Rodríguez, Enhancement of lutein production in *Chlorella sorokiniana* (Chorophyta) by improvement of culture conditions and random mutagenesis, Mar. Drugs 9 (2011) 1607–1624.
[7] M.R. Brown, S.W. Jeffrey, J.K. Volkman, G.A. Dunstan, Nutritional properties of microalgae for mariculture, Aquaculture 151 (1997) 315–331.
[8] P. Spolaore, C. Joannis-Cassan, E. Duran, A. Isambert, Commercial applications of microalgae, J. Biosci. Bioeng. 101 (2006) 87–96.
[9] A. Rehman, A.R. Shakoori, Heavy metal resistance *Chlorella* sp., isolated from tannery effluents, and their role in remediation of hexavalent chromium in industrial waste water, Environ. Contam. Toxicol. 66 (2001) 542–547.
[10] J.R. Benemann, Hydrogen production by microalgae, J. Appl. Phycol. 12 (2000) 291–300.
[11] R. Raja, S. Hemaiswarya, Microalgae and immune potential, Nutr. Health 5 (2010) 515–527.
[12] W. Yongmanitchai, O.P. Ward, Growth of and omega-3 fatty acid production by *Phaeodactylum tricornutum* under different culture conditions, Appl. Environ. Microbiol. 57 (1991) 419–425.
[13] S.M. Renaud, L. Van Thinh, G. Lambrinidis, D.L. Parry, Effect of temperature on growth, chemical composition and fatty acid composition of tropical Australian microalgae grown in batch cultures, Aquaculture 211 (2002) 195–214.
[14] E. Jacob-Lopes, C.H. Gimenes Scoparo, L.M.C. Ferreira Lacerda, T. Teixeira, Franco, Effect of light cycles (night/day) on CO_2 fixation and biomass production by microalgae in photobioreactors, Chem. Eng. Process.: Process Intensification 48 (2009) 306–310.
[15] E. Molina Grima, F.G. Acién Fernández, F. García Camacho, Y. Chisti, Photobioreactors: light regime, mass transfer, and scaleup, J. Biotechnol. 70 (1999) 231–247.
[16] Y.C. Jeon, C.W. Cho, Y.S. Yun, Measurement of microalgal photosynthetic activity depending on light intensity and quality, Biochem. Eng. J. 27 (2005) 127–131.
[17] W. Fu, O. Gudmundsson, A.M. Feist, G. Herjolfsson, S. Brynjolfsson, B.Ø. Palsson, Maximizing biomass productivity and cell density of *Chlorella vulgaris* by using light-emitting diode-based photobioreactor, J. Biotechnol. 161 (2012) 242–249.
[18] .Y.C Wang, C.C. Fu, Y.C. Liu, Effects of using light-emitting diodes on the cultivation of Spirulina platensis, Biochem. Eng. J. 37 (2007) 21–25.
[19] P. Das, W. Lei, S.S. Aziz, J.P. Obbard, Enhanced algae growth in both phototrophic and mixotrophic culture under blue light, Biores. Tech. 102 (2011) 3883–3887.
[20] N. Yeh, J.P. Chung, High-brightness LEDs – energy efficient lighting sources and their potential in indoor plant cultivation, Renew. Sust. Energy Rev. 13 (2009) 2175–2180.
[21] Z. Tukaj, The effects of crude and fuel oils on the growth, chlorophyll 'a' content and dry matter production of a green alga *Scenedesmus quadricauda* (Turp.) bréb, Environ. Pollut. 47 (1987) 9–24.
[22] J.M.S. Rocha, J.E.C. Garcia, M.H.F. Henriques, Growth aspects of the marine microalga Nannochloropsis gaditana, Biomol. Eng. 20 (2003) 237–242.
[23] M.K. Hein, Biological examination, in: Standard Methods for the Examination of Water and Wastewater, American Public Health Association, Washington, 1999, pp. 10-26–10-27.

[24] R.J. Ritchie, Consistent sets of spectrophotometric chlorophyll equations for acetone, methanol and ethanol solvents, Photosynth. Res. 89 (2006) 27–41.
[25] J.M. Heinrich, I. Niizawa, F.A. Botta, A.R. Trombert, H.A. Irazoqui, Stratification of the radiation field inside a photobioreactor during microalgae growth, Photochem. Photobiol. 89 (2013) 1127–1134.
[26] J.M. Heinrich, I. Niizawa, F.A. Botta, A.R. Trombert, H.A. Irazoqui, Analysis, Design of photobioreactors for microalgae production i: method and parameters for radiation field simulation, Photochem. Photobiol. 88 (2012) 938–951.
[27] J.M. Heinrich, I. Niizawa, F.A. Botta, A.R. Trombert, H.A. Irazoqui, Analysis, Design of photobioreactors for microalgae production i: experimental validation of a radiation field simulator based on a Monte Carlo algorithm, Photochem. Photobiol. 88 (2012) 952–960.
[28] www.dled.com.ar
[29] P. Horton, A.V. Ruban, R.G. Walters, Regulation of light harvesting in green plants, Ann Rev. Plant Physiol. Plant Mol. Biol. 47 (1996) 655–684.
[30] D. von Wettstein, S. Gough, C.G. Kannangara, Chlorophyll biosynthesis, Plant Cell 7 (1995) 1039–1057.
[31] S. Bellafiore, F. Barneche, G. Peltier, J.D. Rochaix, State transitions and light adaptation require chloroplast thylakoid protein kinase STN7, Nature 433 (2005) 892–895.
[32] H.W. Heldt, F. Heldt, Plant Biochemistry, Elsevier Academic Press, London, 2005, pp. 67–114.
[33] J.U. Grobbelaar, N. Kurano, Use of photoacclimation in the design of a novel photobioreactor to achieve high yields in algal mass cultivation, J. Appl. Phycol. 15 (2003) 121–126.
[34] A.P. Carvalho, S.O. Silva, J.M. Baptista, F.X. Malcata, Light requirements in microalgal photobioreactors: an overview of biophotonic aspects, Appl. Microbiol. Biotechnol. 89 (2011) 1275–1288.